

Relationships Between Calcium and pH in the Regulation of the Slow Afterhyperpolarization in Cultured Rat Hippocampal Neurons

Tony Kelly and John Church

J Neurophysiol 96:2342-2353, 2006. First published Aug 2, 2006; doi:10.1152/jn.01269.2005

You might find this additional information useful...

This article cites 62 articles, 36 of which you can access free at:

<http://jn.physiology.org/cgi/content/full/96/5/2342#BIBL>

Updated information and services including high-resolution figures, can be found at:

<http://jn.physiology.org/cgi/content/full/96/5/2342>

Additional material and information about *Journal of Neurophysiology* can be found at:

<http://www.the-aps.org/publications/jn>

This information is current as of October 17, 2006 .

Relationships Between Calcium and pH in the Regulation of the Slow Afterhyperpolarization in Cultured Rat Hippocampal Neurons

Tony Kelly and John Church

Department of Cellular and Physiological Sciences, The University of British Columbia, Vancouver, British Columbia, Canada

Submitted 2 December 2005; accepted in final form 19 July 2006

Kelly, Tony and John Church. Relationships between calcium and pH in the regulation of the slow afterhyperpolarization in cultured rat hippocampal neurons. *J Neurophysiol* 96: 2342–2353, 2006. First published August 2, 2006; doi:10.1152/jn.01269.2005. The Ca^{2+} -dependent slow afterhyperpolarization (AHP) is an important determinant of neuronal excitability. Although it is established that modest changes in extracellular pH (pH_o) modulate the slow AHP, the relative contributions of changes in the priming Ca^{2+} signal and intracellular pH (pH_i) to this effect remain poorly defined. To gain a better understanding of the modulation of the slow AHP by changes in pH_o , we performed simultaneous recordings of intracellular free calcium concentration ($[\text{Ca}^{2+}]_i$), pH_i , and the slow AHP in cultured rat hippocampal neurons coloaded with the Ca^{2+} - and pH-sensitive fluorophores fura-2 and SNARF-5F, respectively, and whole cell patch-clamped using the perforated patch technique. Decreasing pH_o from 7.2 to 6.5 lowered pH_i , reduced the magnitude of depolarization-evoked $[\text{Ca}^{2+}]_i$ transients, and inhibited the subsequent slow AHP; opposite effects were observed when pH_o was increased from 7.2 to 7.5. Although decreases and increases in pH_i (at a constant pH_o) reduced and augmented, respectively, the slow AHP in the absence of marked changes in preceding $[\text{Ca}^{2+}]_i$ transients, the inhibition of the slow AHP by decreases in pH_o was correlated with low pH_o -dependent reductions in $[\text{Ca}^{2+}]_i$ transients rather than the decreases in pH_i that accompanied the decreases in pH_o . In contrast, high pH_o -induced increases in the slow AHP were correlated with the accompanying increases in pH_i rather than high pH_o -dependent increases in $[\text{Ca}^{2+}]_i$ transients. The results indicate that changes in pH_o modulate the slow AHP in a manner that depends on the direction of the pH_o change and substantiate a role for changes in pH_i in modulating the slow AHP during changes in pH_o .

INTRODUCTION

In many neurons of the CNS, trains or bursts of action potentials are followed by a prolonged slow afterhyperpolarization (AHP) that, in turn, is an important determinant of subsequent activity (reviewed by Storm 1990; Vogalis et al. 2003). Although the molecular correlate of the apamin-insensitive Ca^{2+} -activated K^+ current that underlies the slow AHP (sI_{ahp}) remains unknown, it is apparent that it can be modulated by a large number of neurotransmitters and second-messenger systems (reviewed by Vogalis et al. 2003; see also Stocker 2004). The slow AHP and sI_{ahp} are also sensitive to changes in extracellular pH (pH_o); decreases and increases in pH_o inhibit and augment, respectively, sI_{ahp} and the slow AHP, with consequent effects on neuronal excitability (Church 1999; Church and McLennan 1989; Kelly and Church 2004). Nevertheless, the relative contributions of changes in the priming

Ca^{2+} signal and intracellular pH (pH_i) to the modulation of sI_{ahp} and the slow AHP by changes in pH_o remain unclear. Changes in pH_o , acting directly or indirectly by changes in pH_i (Church et al. 1998; Tombaugh and Somjen 1996, 1997), could modulate the Ca^{2+} influx through high-voltage-activated (HVA) Ca^{2+} channels constituting the primary source of Ca^{2+} for the activation of the slow AHP in hippocampal neurons (see Shah and Haylett 2000 and references therein). Alternatively, as shown previously for BK-type Ca^{2+} -activated K^+ channels that contribute to the fast AHP that follows a single action potential in hippocampal neurons (Church et al. 1998; see also Kume et al. 1990; Laurido et al. 1991), changes in pH_i consequent on changes in pH_o could affect directly the activities of the Ca^{2+} -activated K^+ channels that underlie the slow AHP.

To distinguish between these possibilities, in the present study we developed a technique in which whole cell perforated patch-clamp recordings of the slow AHP in cultured rat hippocampal neurons were obtained simultaneously with microspectrofluorimetric measurements of both intracellular free calcium concentration ($[\text{Ca}^{2+}]_i$) and pH_i . The results indicate that the slow AHP is sensitive to changes in pH_i and suggest that increases in pH_i make a major contribution to high pH_o -induced increases in the potential. In contrast, a pH_o -dependent reduction in Ca^{2+} influx appears to be the major determinant of the inhibition of the slow AHP observed at low pH_o .

METHODS

Cell preparation

All procedures conformed to guidelines established by the Canadian Council on Animal Care and were approved by The University of British Columbia Animal Care Committee.

Primary cultures of hippocampal neurons were prepared from 2- to 4-day-old postnatal Wistar rats (Animal Care Centre, University of British Columbia). Rat pups were anesthetized with 3% halothane in air and decapitated. Brains were removed rapidly and collected in ice-cold Leibovitz L-15 medium (Invitrogen Canada, Burlington, Canada) supplemented with 34 mM glucose (L-15/G). Hippocampi were removed, collected in ice-cold L-15/G, and then incubated for 15 min at 37°C in L-15/G medium containing 1 mg/ml papain (from papaya latex; Sigma-Aldrich Canada, Oakville, Canada) and 25 $\mu\text{g}/\text{ml}$ DNase (type II from bovine pancreas; Sigma-Aldrich Canada). Afterward, the L-15/G medium was discarded and replaced with Dulbecco's modified Eagle medium F-12 (DMEM/F-12; Invitrogen Canada) supplemented with 29 mM NaHCO_3 and 10% fetal bovine serum (FBS; Sigma-Aldrich Canada) (pH 7.4 at 37°C after equilibration with

Address for reprint requests and other correspondence: J. Church, Department of Cellular and Physiological Sciences, The University of British Columbia, 2350 Health Sciences Mall, Vancouver, B.C., Canada V6T 1Z3 (E-mail: jchurch@interchange.ubc.ca).

The costs of publication of this article were defrayed in part by the payment of page charges. The article must therefore be hereby marked "advertisement" in accordance with 18 U.S.C. Section 1734 solely to indicate this fact.

5% CO₂). Hippocampi were then mechanically dissociated using fire-polished Pasteur pipettes of decreasing tip diameters and the resulting cell suspension was plated at a density of $5\text{--}8 \times 10^5$ neurons/cm² onto 15-mm-diameter glass coverslips coated with poly-D-lysine (100 μg/ml; Sigma-Aldrich Canada) and laminin (16.7 μg/ml; Sigma-Aldrich Canada). Neurons were allowed to adhere to substrate for 2 h before coverslips were transferred into 12 well plates containing DMEM/F-12 supplemented with 29 mM NaHCO₃ and 10% FBS. After 24 h, the growth medium was fully changed to Neurobasal Medium A (Invitrogen Canada) supplemented with B-27 Supplement (Invitrogen Canada), 0.5 mM glutamine (Invitrogen Canada), 50–100 U/ml penicillin (Sigma-Aldrich Canada), and 50–100 μg/ml streptomycin (Sigma-Aldrich Canada). Cultures were fed every 3–4 days by half-changing the existing medium with fresh supplemented Neurobasal Medium A. Glial proliferation was inhibited 48 h after initial plating by adding 10 μM cytosine-β-D-arabino-furanoside hydrochloride (Sigma-Aldrich Canada). Each coverslip consisted primarily of hippocampal neurons with a maximum of 15% cells being glial. Neurons were used 7–14 days after plating.

Solutions and chemicals

The standard bath solution contained (in mM) NaCl 135, KCl 3, NaHCO₃ 21, MgCl₂ 1.5, CaCl₂ 4, D-glucose 10, and HEPES 5 (to increase extracellular buffering capacity and maintain a stable pH_o); pH was 7.2 after equilibration with 5% CO₂-95% air at 30°C. In initial experiments, the bath solution contained 2 mM, rather than 4 mM, CaCl₂; although the effects of increases in pH_o on the magnitudes of depolarization-evoked [Ca²⁺]_i transients and the subsequent slow AHPs were not significantly different at 2 versus 4 mM external Ca²⁺ (see RESULTS), the absolute magnitudes of depolarization-evoked [Ca²⁺]_i transients (50 ± 5 nM, $n = 5$) and the subsequent slow AHPs (1.7 ± 0.1 mV, $n = 5$) at 2 mM external Ca²⁺ under our experimental conditions (i.e., cultured neurons loaded with fura-2 and SNARF-5F) at pH_o 7.2 were small, which effectively precluded the accurate assessment of the inhibitory effects of reductions in pH_{o/i} on the parameters. Therefore we used the approach previously taken by others in hippocampal neurons (e.g., Knöpfel et al. 1990; Segal and Barker 1986) to increase the Ca²⁺ load by increasing external Ca²⁺ to 4 mM and conducted all subsequent experiments under these conditions. Low and high pH solutions contained 3 and 39 mM NaHCO₃ (pH 6.5 and 7.5, respectively, after equilibration with 5% CO₂-95% air); changes in [NaHCO₃] were balanced by equimolar changes in [NaCl]. During perfusion with HCO₃⁻/CO₂-buffered media, the atmosphere in the recording chamber consisted of 5% CO₂-95% air. For nominally HCO₃⁻/CO₂-free medium, HEPES (10 mM) and NaCl isosmotically replaced NaHCO₃ and the solution was titrated with 10 M NaOH to pH 7.2 at 30°C. For Ca²⁺-free medium, CaCl₂ was omitted, [Mg²⁺] was increased to 5.5 mM, and 200 μM EGTA was added. D-(–)-2-Amino-5-phosphonopentanoic acid (D-AP5; 40 μM) and 6-cyano-7-nitroquinoxaline-2,3-dione (CNQX; 20 μM) were present in all bath solutions. Neurons were continuously superfused at a rate of 2 ml/min and all experiments were performed at 30°C.

Salts and experimental compounds, applied by superfusion, were obtained from Sigma-Aldrich Canada, with the exceptions of potassium methylsulfate (ICN Pharmaceuticals Canada, Montreal, Canada), the AM forms of fura-2 and seminaphthorhodafuor-5F 5-(and-6)-carboxylic acid (SNARF-5F; Molecular Probes, Eugene, OR), D-AP5 and CNQX (Tocris Bioscience, Ellisville, MO), and UCL 2027 (a generous gift from Drs. C. R. Ganellin and D. G. Haylett, Departments of Chemistry and Pharmacology, respectively, University College London, London, UK).

Microspectrofluorimetry

Concurrent measurements of [Ca²⁺]_i and pH_i were performed using the ratiometric indicators fura-2 and SNARF-5F, respectively. As

detailed by Martínez-Zaguilán et al. (1996b), the excitation and emission characteristics of fura-2 and SNARF derivatives are sufficiently distinct to permit the accurate discrimination of [Ca²⁺]_i- and pH_i-dependent signals from dual dye-loaded cells (see also Sheldon et al. 2004a). Neurons were incubated with 0.5–10 μM (see RESULTS) fura-2-AM for 30 min at 32°C in the presence of 0.04% Pluronic F-127; 10 μM SNARF-5F-AM was added during the final 10 min of incubation. After loading, coverslips were placed in standard medium for 20 min to ensure deesterification of the fluorophores and then mounted in a temperature-controlled perfusion chamber to form the base of the chamber.

Measurements of bulk cytosolic [Ca²⁺]_i and pH_i were performed at the somatic level using the dual-excitation and dual-emission ratio methods, respectively, using an imaging system (Atto Bioscience, Rockville, MD) in conjunction with an Axiovert 135 epifluorescence microscope (Carl Zeiss Canada, Don Mills, ON) equipped with two intensified charge-coupled device cameras (Atto Bioscience). A detailed description of the optical equipment used was previously presented (Sheldon et al. 2004a). In brief, as illustrated in Fig. 1, fura-2-derived fluorescence emission intensities from regions of interest placed on a patch-clamped neuron and neighboring intact (i.e., not patch-clamped) neurons on the same coverslip were measured with a single camera at 550 ± 40 nm during excitation at 334 ± 5 nm and then at 380 ± 5 nm; the excitation wavelength was then changed to 488 ± 5 nm and SNARF-5F-derived fluorescence emissions were split by a dichroic mirror centered at 605 nm and measured by two separate cameras at 550 ± 40 and 640 ± 20 nm. Camera registration was confirmed before every experiment. Fura-2- and SNARF-5F-derived ratio pairs were collected continuously by alternating between the dual-excitation and dual-emission modes; each automated cycle took about 1.5 s to complete, including a <0.5-s delay between collecting fura-2- and SNARF-5F-derived ratio pairs, and was repeated every 2–15 s (typically 10 s) during the course of an experiment; during the recording of depolarization-evoked [Ca²⁺]_i transients, the acquisition of pH data was interrupted and fura-2-derived ratio pairs only were collected every 0.6–0.8 s.

A one-point calibration technique was used to convert background-corrected SNARF-5F-derived emission intensity ratio values (BI_{550}/BI_{640}) into pH_i values, as described (Baxter and Church 1996; Sheldon et al. 2004a). In brief, neurons loaded with SNARF-5F and fura-2 were exposed at the end of an experiment to a pH 7.00 high-[K⁺] solution containing 10 μM nigericin and the resulting background-corrected ratio value at pH_i 7.00 in a given neuron was used as a normalization factor for the BI_{550}/BI_{640} ratio values obtained from that neuron during that experiment. SNARF-5F-derived BI_{550}/BI_{640} ratio values obtained during the one-point calibration procedure were not significantly different in patch-clamped (1.77 ± 0.04 ratio units; $n = 6$ neurons) versus neighboring intact (i.e., not patch-clamped) neurons on the same coverslips (1.69 ± 0.05 ratio units; $n = 6$ neuronal populations). The parameters required to convert experimentally derived BI_{550}/BI_{640} ratio values into pH_i values were determined in full calibration experiments in which neurons were exposed to 10 μM nigericin-containing high-[K⁺] media titrated to pH 5.5–8.5 in 0.5 pH unit increments (see Sheldon et al. 2004a); no differences in SNARF-5F calibration parameters were observed between neurons loaded with SNARF-5F alone or coloaded with SNARF-5F and fura-2 (data not shown; see also Sheldon et al. 2004a).

The parameters required to convert experimentally derived background-corrected fura-2-derived emission intensity ratio values (BI_{334}/BI_{380}) into [Ca²⁺]_i values were determined in full in situ calibration experiments, as described in detail by Martínez-Zaguilán et al. (1991, 1996a,b). In brief, neurons loaded with fura-2 and SNARF-5F were exposed to K⁺-EGTA/Ca²⁺-EGTA buffers containing 10 μM 4-BrA23187 and 10 μM nigericin at three different pH values (pH 6.5–7.5 in 0.5 pH unit increments) with variable free Ca²⁺ concentrations (range 0–500 μM). Data from these experiments were used to obtain the calibration parameters that describe the effects of

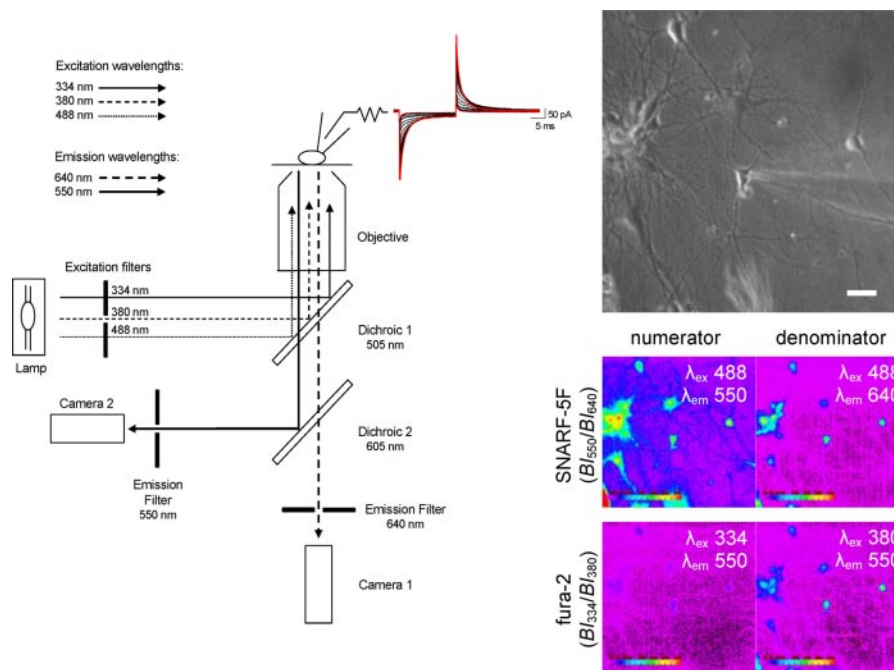


FIG. 1. Schematic representation of the recording system. *Left*: diagram of the optical equipment used to measure the intracellular free calcium concentration ($[Ca^{2+}]_i$) and intracellular pH (pH_i) simultaneously in neurons patch-clamped using the amphotericin B perforated patch-clamp technique (adapted from Sheldon et al. 2004a). Neurons were excited with light provided by a 100-W Hg lamp and band-pass filtered at 488 ± 5 nm (for SNARF-5F) or alternately at 334 ± 5 and 380 ± 5 nm (for fura-2). Filtered excitation light was reflected by a 505-nm dichroic mirror (Dichroic 1), passed through a $\times 40$ LD Achromplan objective, and illuminated neurons loaded with fluorophores. Fura-2 fluorescence emissions passed through Dichroic 1, were reflected by a dichroic mirror centered at 605 nm (Dichroic 2), passed through a 550 ± 40 nm band-pass emission filter, and were detected by Camera 2. Fluorescence emissions from SNARF-5F passed through Dichroic 1, were split by Dichroic 2, and passed through 640 ± 20 - or 550 ± 40 -nm band-pass emission filters before being detected by Cameras 1 and 2, respectively. After the formation of a $G\Omega$ seal, there was a progressive increase in the magnitudes of the capacitance transients; perforated patch recordings were performed when the access resistance stabilized at <50 M Ω . *Right*: phase-contrast photomicrograph of a field of cultured hippocampal neurons; the pyramidal neuron near the center was patch-clamped (the patch pipette is visible). Scale bar: 20 μ m. Below are shown pseudocolored fluorescence emissions from the neurons coloaded with SNARF-5F and fura-2 and illuminated sequentially at the indicated excitation wavelengths (λ_{ex}). Intensities of emitted fluorescence (λ_{em}) were measured at either 550 or 640 nm. In any given experiment, $[ion]_i$ measurements were made from both the patch-clamped neuron and the intact (i.e., not patch-clamped) neighboring neurons on the same coverslip.

pH on the affinity of fura-2 for Ca^{2+} (see Martínez-Zaguilán et al. 1991, 1996a,b). Subsequently, the steady-state pH_i value measured immediately before an evoked $[Ca^{2+}]_i$ transient was used to correct for the effect of pH on the K_d , R_{min} , and R_{max} of fura-2, and $[Ca^{2+}]_i$ was calculated from the equation

$$[Ca^{2+}]_i = K_{d, pH\ corr} [(R - R_{min, pH\ corr}) / (R_{max, pH\ corr} - R)] \quad (1)$$

where $K_{d, pH\ corr}$ is the pH-corrected K_d of fura-2 for Ca^{2+} , R is the experimentally derived background-corrected fura-2 ratio value, and $R_{min, pH\ corr}$ and $R_{max, pH\ corr}$ are the minimum and maximum ratio values, respectively, corrected for pH (Martínez-Zaguilán et al. 1991, 1996a,b; see also Church et al. 1998).

To limit potential cross-contamination by nigericin, perfusion lines were replaced and the imaging chamber was decontaminated after each experiment by soaking first in ethanol, then in 20% Decon 75 (BDH, Toronto, Canada) and rinsing vigorously with water.

Electrophysiology

Because conventional whole cell recordings are associated with a rapid and marked rundown of the slow AHP in cultured hippocampal neurons, we used the amphotericin B perforated patch-clamp technique described by Shah and Haylett (2000) to measure membrane potential (V_m) and the slow AHP in neurons loaded with fura-2 and SNARF-5F. Patch pipettes were pulled from 1.2 mm OD \times 0.9 mm ID borosilicate tubing (World Precision Instruments, Sarasota, FL). The first 100- to 200- μ m section of the pipette tip was filled with a

standard solution containing (in mM) KMeSO₄ 145, KCl 10, and HEPES 10 (titrated to pH 7.4 with 6 mM KOH) and then backfilled with the same solution but containing 1.2 mg/ml amphotericin B; final osmolality was about 290 mOsm/kg H₂O and open pipette resistance when filled was 2–5 M Ω . The reference bath electrode was a 3 M KCl, 4% agar bridge. After a seal >1 G Ω was achieved, recordings were made (Axoclamp 2 or Axopatch 200B, Axon Instruments, Union City, CA) when access resistance was stable at <50 M Ω . Current and voltage waveforms were low-pass filtered at 3 kHz and digitized at 5–10 kHz using a Digidata 1322A controlled by pCLAMP software (v.8, Axon Instruments).

During current-clamp recordings, a train of action potentials evoked by 4-ms suprathreshold depolarizing current pulses applied at 33 or 50 Hz (Master-8, A.M.P.I., Jerusalem, Israel) was used to generate a $[Ca^{2+}]_i$ transient and the subsequent slow AHP; the number of action potentials in the train was held the same under control and test conditions. Under voltage-clamp conditions, a 80- to 200-ms depolarizing voltage step from the holding potential (-50 mV) to 0–20 mV was used to elicit a $[Ca^{2+}]_i$ transient and the subsequent sI_{ahp} ; leakage currents (estimated using 10-mV, 100-ms hyperpolarizing voltage steps from -50 mV) were subtracted off-line from all records of sI_{ahp} . The criteria for detecting whether perforated patch recordings broke through included a change in the measured access resistance, an increase in the leakage current (which was estimated in all experiments), a sudden loss of fura-2 and SNARF-5F fluorescence from the patched cell, and, finally, a rapid rundown of the slow AHP itself (see Shah and Haylett 2000).

Data analysis

The change in pH_i evoked by a test maneuver was quantified as the difference between the steady-state pH_i value observed under the test condition with the mean of the steady-state pH_i values observed just before and, whenever possible, after full recovery from the test condition. In any given patch-clamped neuron, trains of 13 action potentials (see RESULTS) elicited $[\text{Ca}^{2+}]_i$ transients of consistent amplitude, which were quantified as the difference between the BI_{334}/BI_{380} ratio value (or $[\text{Ca}^{2+}]_i$) measured immediately before the train of action potentials and the peak BI_{334}/BI_{380} ratio value (or peak $[\text{Ca}^{2+}]_i$) observed during the transient. In light of the relatively slow rates at which fura-2-derived ratio pairs were acquired, the computed means of two to five $[\text{Ca}^{2+}]_i$ transients obtained before, during, and, whenever possible, after exposure to a test solution were used to quantify the effects of a test maneuver on the amplitudes of depolarization-evoked $[\text{Ca}^{2+}]_i$ transients.

Experimentally induced changes in the slow AHP were quantified as the difference between the computed mean of the peak amplitudes of the slow AHPs evoked under a test condition with the mean of the slow AHP amplitudes evoked before and, whenever possible, after recovery from the test condition. If a distinct peak in the slow AHP was observed under control conditions, the amplitudes of the slow AHPs under test/wash conditions were measured at the same time interval after the end of the train of action potentials. If a distinct peak in the slow AHP was not evident under control conditions, slow AHP amplitude was measured 700 ms after the end of the train of action potentials (i.e., at a time point at which the slow AHP is usually near its peak and the medium AHP, if present, has decayed by >90%; see Kelly and Church 2004; Shah and Haylett 2000); measurements of the slow AHP under test/wash conditions were then made at the same time interval. Test measurements were conducted at the original control membrane potential by passing, when necessary, steady current through the recording electrode. Experimentally induced changes in sI_{ahp} were quantified by comparing the peak amplitudes of the current obtained under control/wash and test conditions (see Kelly and Church 2004).

Data are presented as means \pm SE, with the accompanying n value referring to either the number of patch-clamped neurons (each on a different coverslip) or, for neighboring intact (i.e., not patch-clamped) neurons on the same coverslips, the number of coverslips (i.e., neuronal populations) from which data were obtained. Data were analyzed in pCLAMP v.8 or Origin v.7 (OriginLab, Northampton, MA). Unless otherwise noted, statistical comparisons were performed using Student's two-tailed t -test, paired or unpaired as appropriate. In Figs. 5B, 6B, 8C, and 8D, the Pearson product-moment correlation coefficient was used to determine whether the change in the $[\text{Ca}^{2+}]_i$,

transient and/or the change in pH_i evoked by a given experimental maneuver was related to the change in the slow AHP, and the significance of the correlation was assessed using the t -test (see Glantz 2002). In all cases, statistical significance was assumed at the 5% level.

RESULTS

Fura-2 loading

Fura-2, a BAPTA derivative, chelates Ca^{2+} and thereby could modulate the Ca^{2+} -dependent slow AHP (e.g., Abel et al. 2004; Helmchen et al. 1996; Lancaster and Batchelor 2000; Lasser-Ross et al. 1997). Initially, therefore, we examined the effects of different concentrations of fura-2-AM in the loading medium on depolarization-evoked $[\text{Ca}^{2+}]_i$ transients and the incidence of the slow AHP under our experimental conditions.

Under control pH_o 7.2 $\text{HCO}_3^-/\text{CO}_2$ -buffered conditions in the absence of fluorophores, resting V_m was -60 ± 1 mV, input resistance (R_{in}) was 488 ± 11 M Ω , and a train of 13 action potentials (see following text) was followed by a slow AHP in 11/20 neurons (Table 1). A medium AHP was seen in only a minority (4/11) of cells that exhibited a slow AHP (see also Shah and Haylett 2000) and was not further analyzed. Voltage-clamp recordings performed on five neurons that exhibited a slow AHP under current-clamp conditions revealed that a 80- to 200-ms depolarizing step from -50 to 0 – 20 mV elicited an $sI_{\text{ahp}} \geq 40$ pA in only 40% of these neurons (currents < 40 pA at pH_o 7.2 were considered too small for reliable analysis under our experimental conditions). Although the overall incidence of sI_{ahp} observed here is lower than that reported by Shah and Haylett (2000), who found that 50–60% of their cultured hippocampal neurons exhibited a $sI_{\text{ahp}} > 20$ pA, it is consistent with the findings of Alger et al. (1994) in the same cell type. In light of these observations, the majority of subsequent experiments examined the slow AHP under current-clamp conditions.

In 12 of 16 neurons loaded with 2–10 μM fura-2-AM, a train of 13 action potentials elicited a transient increase in the fura-2-derived BI_{334}/BI_{380} ratio value; the remaining cells failed to exhibit an increase in $[\text{Ca}^{2+}]_i$. Of those cells that displayed a $[\text{Ca}^{2+}]_i$ transient, only 25% exhibited a slow AHP, the peak amplitude of which was significantly smaller than that

TABLE 1. Effects of fluorophore loading on depolarization-evoked $[\text{Ca}^{2+}]_i$ transients and subsequent slow AHPs

Loading Condition	n	$[\text{Ca}^{2+}]_i$ Transient		Slow AHP	
		Incidence, %	Peak amplitude, BI_{334}/BI_{380} ratio units	Incidence, %	Peak amplitude, mV
No fluorophore	20	n.a.	n.a.	55	5.3 ± 0.2
Fura-2-AM					
2–10 μM	16	75	0.08 ± 0.01	25	1.5 ± 0.5^a
0.5–1 μM	14	100	0.18 ± 0.01^b	64	$5.1 \pm 0.3^{b,c}$
Fura-2-AM (0.5–1 μM) + SNARF-5F-AM (10 μM)	72	100	$0.19 \pm 0.01^{b,d}$	58	$4.7 \pm 0.3^{b,c,d}$

Values are means \pm SE; n = total number of perforated patch-clamped neurons examined under each experimental condition. In all cases, a train of 13 action potentials was used to evoke a $[\text{Ca}^{2+}]_i$ transient and subsequent slow AHP. Concentrations of fluorophores indicated are those in the loading medium. Incidence of $[\text{Ca}^{2+}]_i$ transient is the percentage of the total number of fura-2-loaded neurons examined that displayed a $[\text{Ca}^{2+}]_i$ transient. Incidence of slow AHP is either the percentage of neurons not loaded with a fluorophore that displayed a slow AHP or the percentage of those fura-2-loaded cells that displayed a $[\text{Ca}^{2+}]_i$ transient and a subsequent slow AHP. $^aP < 0.01$ compared with the respective value obtained in the absence of fura-2. $^bP < 0.01$ compared with the respective values obtained in cells loaded with 2–10 μM fura-2. $^cP > 0.7$ compared with the respective value obtained in the absence of fluorophores. $^dP > 0.7$ compared with the respective values obtained in cells loaded with 0.5–1 μM fura-2 in the absence of SNARF-5F. n.a., not applicable.

observed in the absence of fura-2 (Table 1). In contrast, in each of 14 neurons loaded with 0.5–1 μM fura-2-AM, the same stimulus elicited an increase in BI_{334}/BI_{380} ratio values that was significantly larger than observed in neurons loaded with $\geq 2 \mu\text{M}$ fura-2-AM, and in 64% of these cells the $[\text{Ca}^{2+}]_i$ transient was followed by a slow AHP that was not significantly different from that observed in the absence of fura-2 (Table 1). Finally, in 72 cells loaded with $\leq 1 \mu\text{M}$ fura-2-AM, additional loading with 10- μM SNARF-5F-AM failed to significantly affect the amplitude of depolarization-evoked $[\text{Ca}^{2+}]_i$ transients or the incidence and amplitude of the subsequent slow AHP (Table 1), which remained stable for the duration of the recordings (typically 30–40 min). Consequently, subsequent experiments were performed in neurons coloaded with 10 μM SNARF-5F-AM and $\leq 1 \mu\text{M}$ fura-2-AM.

Simultaneous measurements of V_m , $[\text{Ca}^{2+}]_i$, and pH_i

In 42 neurons loaded with 10 μM SNARF-5F-AM and $\leq 1 \mu\text{M}$ fura-2-AM, resting V_m and R_{in} under control pH_o 7.2 $\text{HCO}_3^-/\text{CO}_2$ -buffered conditions were $-59 \pm 0.3 \text{ mV}$ and $474 \pm 18 \text{ M}\Omega$, respectively ($P > 0.6$ in each case, compared with respective values obtained in the absence of fluorophores; see above). Resting pH_i in perforated patch-clamped cells (pH_i 7.19 ± 0.01 ; $n = 42$ neurons) was not significantly different ($P > 0.3$) from that measured in neighboring intact (i.e., not patch-clamped) neurons on the same coverslips (pH_i 7.23 ± 0.01 ; $n = 42$ coverslips) and was consistent with values previously reported in intact cultured fetal (Baxter and Church 1996) and acutely isolated adult (Bevensee et al. 1996; Brett et al. 2002) rat hippocampal neurons in the presence of HCO_3^- . Also as reported previously for intact hippocampal neurons under $\text{HCO}_3^-/\text{CO}_2$ -buffered conditions (Baxter and Church 1996; Bevensee et al. 1996; Brett et al. 2002; Smith et al. 1998), the distributions of resting pH_i values in both perforated patch-clamped and intact neurons were unimodal, albeit the distribution was slightly skewed in patch-clamped cells (Fig. 2A). As illustrated in Fig. 2B, resting fura-2-derived BI_{334}/BI_{380} ratio values were significantly ($P < 0.05$) higher in patch-clamped neurons (0.32 ± 0.01 ratio units; $n = 42$ neurons) than in neighboring intact neurons on the same coverslips (0.26 ± 0.01 ratio units; $n = 42$ coverslips), although both values were within the range observed previously in intact cultured hippocampal neurons with our recording system (e.g., Church et al. 1994, 1998).

Next, given the relative paucity of studies in which the slow AHP has been examined in neurons in primary culture (see Segal and Barker 1986; Shah and Haylett 2000; Shah et al. 2001), we performed a limited series of experiments to assess the characteristics of the slow AHP under our experimental conditions. Consistent with previous findings in hippocampal neurons in slices and in culture (e.g., Gerlach et al. 2004; Lancaster and Batchelor 2000; Shah and Haylett 2000; Wu et al. 2004; see also Abel et al. 2004), the peak amplitudes of $[\text{Ca}^{2+}]_i$ transients and the subsequent slow AHPs increased with the number of action potentials in the stimulus train, the latter reaching a maximum in at least nine action potentials (Fig. 3, A and C); trains of just subthreshold depolarizations failed to elicit $[\text{Ca}^{2+}]_i$ transients (Fig. 3B) or slow AHPs. Under the present experimental conditions, neither a train of 13 action potentials nor membrane depolarization from -50 to 20

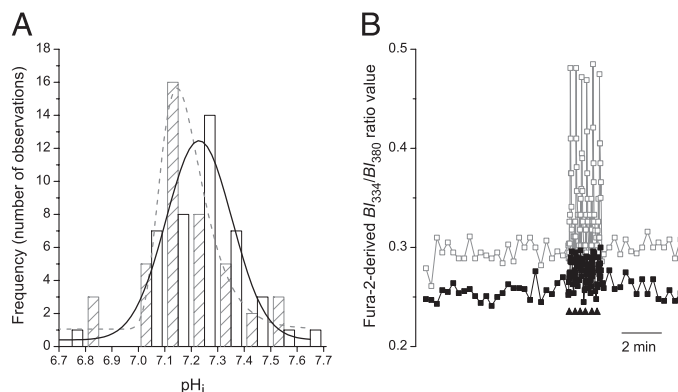


FIG. 2. Resting pH_i and $[\text{Ca}^{2+}]_i$ in perforated patch-clamped and intact hippocampal neurons loaded with $\leq 1 \mu\text{M}$ fura-2-AM and 10 μM SNARF-5F-AM. *A*: frequency histograms of steady-state pH_i values for perforated patch-clamped and neighboring intact (i.e., not patch-clamped) neurons on the same coverslips under control extracellular pH (pH_o) 7.2 $\text{HCO}_3^-/\text{CO}_2$ -buffered conditions. Distribution of steady-state pH_i values in intact neurons (open bars; $n = 42$ coverslips) was fitted best ($r^2 = 0.91$) with a single Gaussian distribution (solid line) with a mean at pH_i 7.23 ± 0.01 . Distribution of steady-state pH_i values in patch-clamped neurons (hatched bars; $n = 42$ neurons) was slightly skewed and was fitted best ($r^2 = 0.85$) with an asymmetric logistic function (dashed line) with a modal value at pH_i 7.17. *B*: resting fura-2-derived BI_{334}/BI_{380} ratio values (representing $[\text{Ca}^{2+}]_i$) were slightly higher in a perforated patch-clamped neuron (\square), compared with a neighboring intact neuron on the same coverslip (\blacksquare). Six trains of action potentials (each train consisting of 13 action potentials delivered at 33 Hz; \blacktriangle) elicited transient increases in $[\text{Ca}^{2+}]_i$ of consistent amplitude in only the patch-clamped neuron.

mV for ≤ 2 s evoked measurable changes in pH_i , although decreases in pH_i consistent with the activation of the plasmalemmal $\text{Ca}^{2+},\text{H}^+$ -ATPase (Trapp et al. 1996; Willoughby and Schwiening 2002) were observed if the membrane was depolarized for >5 s (data not shown). Therefore in subsequent experiments, a train of 13 action potentials was used to generate a $[\text{Ca}^{2+}]_i$ transient and the effects of experimental maneuvers were examined on this transient and the subsequent slow AHP.

Finally, consistent with previous reports in hippocampal pyramidal neurons (e.g., Sah and Clements 1999; Shah and Haylett 2000), the amplitudes of depolarization-evoked $[\text{Ca}^{2+}]_i$ transients and the subsequent slow AHPs were significantly reduced under external Ca^{2+} -free conditions (not shown) or by the application of 200 μM Cd^{2+} (Fig. 4). In contrast, 10 μM isoproterenol and 5–10 μM UCL 2027 (a relatively selective inhibitor of the slow AHP in rat hippocampal neurons; Shah et al. 2001) significantly reduced the slow AHP but not the preceding $[\text{Ca}^{2+}]_i$ transient (Fig. 4).

Effects of a decrease in pH_o

Under control pH_o 7.2 $\text{HCO}_3^-/\text{CO}_2$ -buffered conditions, resting pH_i in intact and perforated patch-clamped neurons loaded with 10 μM SNARF-5F and $\leq 1 \mu\text{M}$ fura-2 was 7.30 ± 0.02 ($n = 8$ coverslips) and 7.31 ± 0.02 ($n = 8$ neurons; Fig. 5A), respectively. In the patch-clamped neurons, resting $[\text{Ca}^{2+}]_i$ was $70 \pm 5 \text{ nM}$ and a train of 13 action potentials elicited a $120 \pm 8 \text{ nM}$ increase in $[\text{Ca}^{2+}]_i$; the amplitude of the subsequent slow AHP was $4.4 \pm 0.2 \text{ mV}$ (Fig. 5A). Reducing pH_o from 7.2 to 6.5 produced significant ($P > 0.01$ in both cases) reductions in pH_i in both patch-clamped cells (to pH_i 7.10 ± 0.03 ; Fig. 5A) and the neighboring intact cells on the same

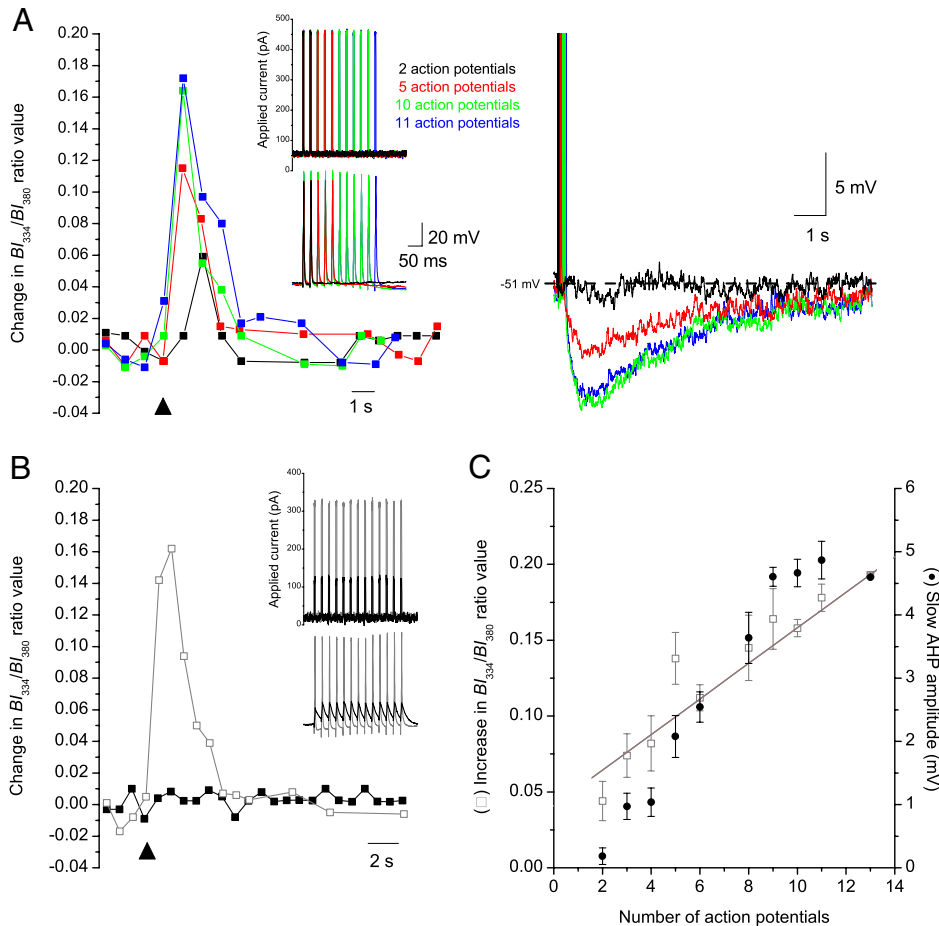


FIG. 3. Depolarization-evoked $[Ca^{2+}]_i$ transients and subsequent slow afterhyperpolarizations (AHPs). *A*: under control pH_o 7.2 HCO_3^-/CO_2 -buffered conditions, the injection of 2–11 suprathreshold 4-ms depolarizing current pulses, applied at 33 Hz, elicited trains of 2–11 action potentials (*inset*). Each train of action potentials (applied at \blacktriangle) evoked a $[Ca^{2+}]_i$ transient (*left*, represented by changes in fura-2–derived BI_{334}/BI_{380} ratio values) that was followed by a slow AHP (*right*). *B*: in a different neuron, the injection of 13 subthreshold 4-ms depolarizing current pulses, applied at 33 Hz, failed to elicit action potentials or a $[Ca^{2+}]_i$ transient (\blacksquare); increasing the amplitude of the current pulse led to the development of a train of action potentials and a distinct $[Ca^{2+}]_i$ transient (\square). *C*: peak amplitude of the $[Ca^{2+}]_i$ transient (\square) increased linearly with the number of action potentials in the stimulus train, whereas the peak amplitude of the associated slow AHP (\bullet) reached a maximum at ≥ 9 action potentials. Values are plotted as means \pm SE of data obtained from ≥ 3 neurons in all cases; error bars for data points obtained with 13 action potentials are within the symbol areas. Straight line is a linear least-squares regression fit ($r^2 = 0.90$) to the data points indicated by *.

coverslips (to pH_i 7.10 ± 0.04). In agreement with previous findings (Church et al. 1998), reducing pH_o from 7.2 to 6.5 failed to significantly affect resting $[Ca^{2+}]_i$ (data not shown); in contrast, in the patch-clamped neurons, the peak amplitudes of the $[Ca^{2+}]_i$ transients and the subsequent slow AHPs declined to 55 ± 3 nM (a $51 \pm 2\%$ reduction) and 0.9 ± 0.1 mV (a $79 \pm 2\%$ reduction), respectively ($P < 0.01$ in both cases, compared with the respective values obtained at pH_o 7.2; Fig. 5A). Recovery of pH_i and the amplitudes of the $[Ca^{2+}]_i$ transients and slow AHPs from the effects of exposure to pH 6.7 medium was slow and usually incomplete. In one cell in which a distinct sI_{ahp} was discernable, the peak amplitude of sI_{ahp} declined by 73%, from 95 pA at pH_o 7.2 to 25 pA at pH_o 6.5.

The reductions in pH_i and the percentage reductions in the peak amplitudes of the $[Ca^{2+}]_i$ transients observed in patch-clamped cells on reducing pH_o from 7.2 to 6.5 were then plotted against the percentage reductions in the peak amplitudes of the slow AHPs measured in the same cells (Fig. 5B). The percentage reduction in the slow AHP at pH_o 6.5 was significantly correlated with the percentage reduction in the magnitude of the depolarization-evoked $[Ca^{2+}]_i$ transient but not with the reduction in pH_i ($P < 0.01$ and $P = 0.17$, respectively). The lack of a significant correlation between the reductions in the slow AHP and pH_i was maintained when the reduction in pH_i was plotted as an increase in $[H^+]_i$ or a percentage increase in $[H^+]_i$ (not shown; see Fig. 8D).

Effects of an increase in pH_o

Under pH_o 7.2 HCO_3^-/CO_2 -buffered conditions, resting pH_i in perforated patch-clamped and intact, unpatched neighboring neurons on the same coverslips was 7.22 ± 0.01 ($n = 16$ neurons; Fig. 6A) and 7.24 ± 0.02 ($n = 16$ coverslips), respectively ($P > 0.2$ in both cases, compared with the values observed in the preceding experimental series also at pH_o 7.2). In the patch-clamped neurons, resting $[Ca^{2+}]_i$ was 80 ± 2 nM and a train of 13 action potentials elicited a 94 ± 3 nM increase in $[Ca^{2+}]_i$ and a subsequent slow AHP, the peak amplitude of which was 3.3 ± 0.1 mV (Fig. 6A). Increasing pH_o from 7.2 to 7.5 significantly ($P < 0.01$ in both cases) increased pH_i in patch-clamped and intact neurons to 7.34 ± 0.01 (Fig. 6A) and 7.35 ± 0.02 pH units, respectively. In the patch-clamped neurons, high pH_o conditions failed to affect resting $[Ca^{2+}]_i$ (see also Church et al. 1998) but significantly ($P < 0.01$ in both cases) increased the peak amplitudes of the $[Ca^{2+}]_i$ transient to 130 ± 4 nM (a $36 \pm 1\%$ increase) and the subsequent slow AHP to 5.3 ± 0.2 mV (a $69 \pm 2\%$ increase) (Fig. 6A). Similar results were obtained at 2 mM external Ca^{2+} , where increasing pH_o from 7.2 to 7.5 increased the amplitude of the $[Ca^{2+}]_i$ transient evoked by 13 action potentials by $32 \pm 2\%$ ($n = 3$) and the amplitude of the subsequent slow AHP by $85 \pm 4\%$ ($P > 0.02$ in each case, compared with the increases observed at 4 mM $[Ca^{2+}]_o$). In addition, similar to the slow AHP and sI_{ahp} observed during conventional whole cell recordings in rat CA1 neurons in slices (Kelly and Church 2004), the augmented

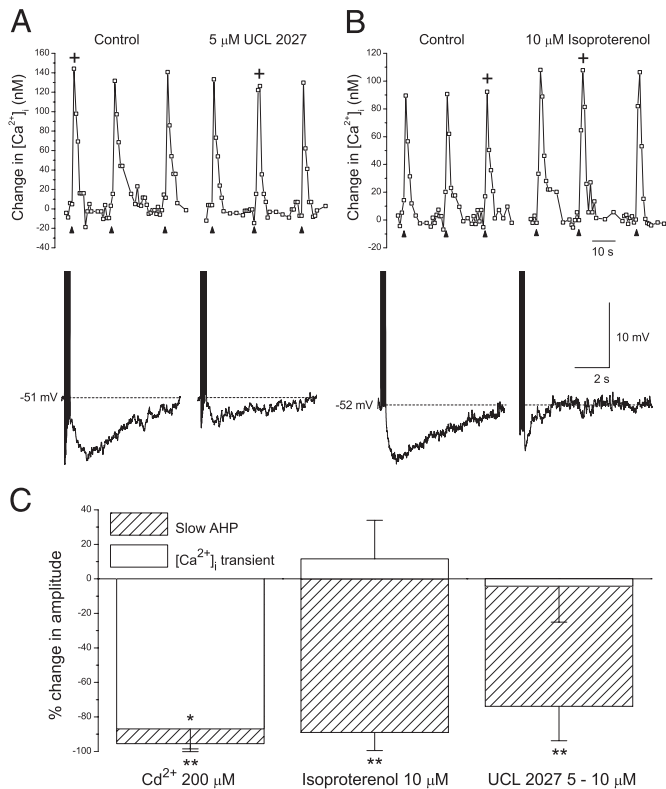


FIG. 4. Pharmacological characterization of depolarization-evoked $[\text{Ca}^{2+}]_i$ transients and subsequent slow AHPs. *A* and *B*: simultaneous $[\text{Ca}^{2+}]_i$ and perforated patch-clamp recordings from 2 different cultured hippocampal neurons. Under control pH_o 7.2 $\text{HCO}_3^-/\text{CO}_2$ -buffered conditions, trains of 13 action potentials (applied at \blacktriangle) elicited $[\text{Ca}^{2+}]_i$ transients (*top*) that were followed by slow AHPs (*bottom*). In this and subsequent figures, the $[\text{Ca}^{2+}]_i$ transients used to elicit the slow AHPs shown are indicated by +. Application of 5 μM UCL 2027 (*A*) or 10 μM isoproterenol (*B*) reduced the slow AHP without appreciably affecting the preceding $[\text{Ca}^{2+}]_i$ transient. Scale bars in *B* apply to the respective traces in *A*. *C*: summary of the mean \pm SE percentage changes in the peak amplitudes of $[\text{Ca}^{2+}]_i$ transients and the subsequent slow AHPs observed under the conditions indicated on the figure, compared with the peak amplitudes obtained under control conditions. $n \geq 3$ in all cases. * $P < 0.05$ and ** $P < 0.01$ for the difference between the corresponding measurement obtained in the absence vs. presence of the indicated compound.

slow AHP observed on increasing pH_o from 7.2 to 7.5 was insensitive to 100 nM apamin (in three cells, slow AHP amplitude at pH_o 7.5 was 5.5 ± 0.6 and 5.5 ± 0.3 mV in the absence and presence of apamin, respectively; $P > 0.9$) but declined from 5.5 ± 0.6 to 0.7 ± 0.2 mV ($n = 3$) in the presence of 10 μM isoproterenol (an $87 \pm 4\%$ reduction; $P < 0.05$; see also Fig. 4C). In two cells in which a distinct sI_{ahp} was apparent, the peak amplitude of sI_{ahp} increased by 51%, from 52 pA at pH_o 7.2 to 79 pA at pH_o 7.5 ($P < 0.05$).

The percentage increases in the peak amplitudes of $[\text{Ca}^{2+}]_i$ transients and the increases in pH_i observed on raising pH_o from 7.2 to 7.5 in individual perforated patch-clamped neurons were then plotted against the percentage increases in the peak amplitudes of the slow AHPs measured in the same cells (Fig. 6B). In contrast to results obtained on reducing pH_o to 6.5, the high pH_o -induced increase in the peak amplitude of the slow AHP was significantly correlated with the increase in pH_i ($P < 0.01$) rather than the increase in the peak amplitude of the preceding $[\text{Ca}^{2+}]_i$ transient ($P = 0.26$). Similar conclusions were reached when the increase in pH_i was plotted as a

decrease in $[\text{H}^+]_i$ or a percentage decrease in $[\text{H}^+]_i$ (not shown; see Fig. 8D).

Effects of changing pH_i at a constant pH_o

Next, we examined whether changes in pH_i at a constant pH_o affect the magnitudes of depolarization-evoked $[\text{Ca}^{2+}]_i$ transients and the subsequent slow AHPs. Although externally applied weak acids (e.g., propionic acid, butyric acid) and weak bases (e.g., NH_3 , trimethylamine) are widely used to

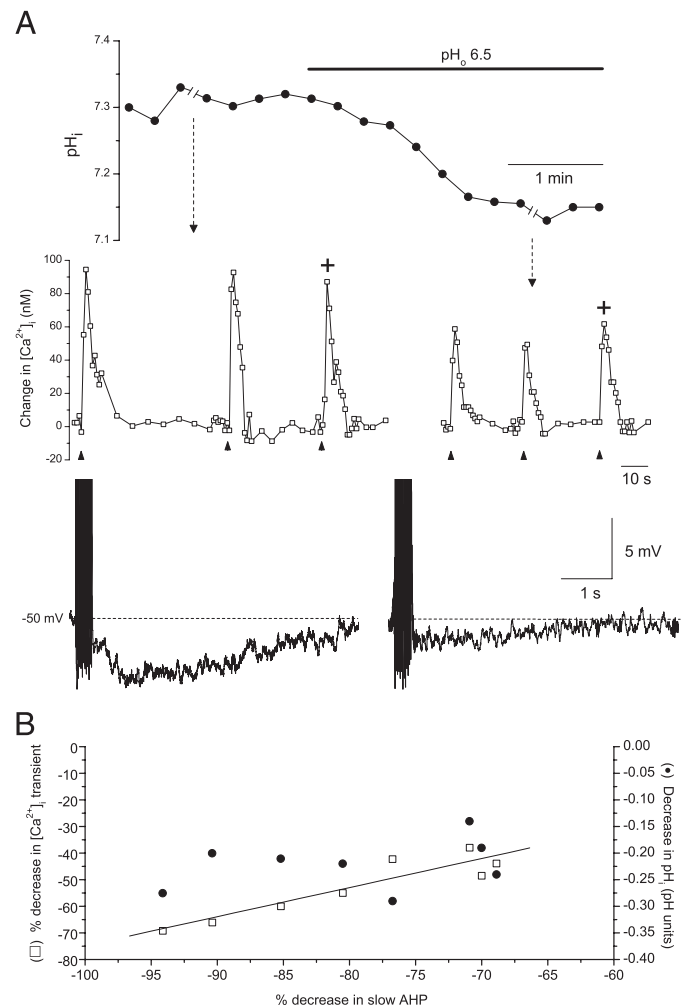


FIG. 5. Effects of a decrease in pH_o on pH_i , $[\text{Ca}^{2+}]_i$ transients, and the slow AHP. *A*: simultaneous measurements of pH_i (*top*), $[\text{Ca}^{2+}]_i$ (*middle*), and V_m (*bottom*) from a perforated patch-clamped hippocampal neuron under $\text{HCO}_3^-/\text{CO}_2$ -buffered conditions. Decreasing pH_o from 7.2 to 6.5 reduced pH_i . Peak amplitudes of $[\text{Ca}^{2+}]_i$ transients (evoked by trains of 13 action potentials applied at \blacktriangle) and the subsequent slow AHPs were reduced at pH_o 6.5 compared with pH_o 7.2. Breaks in the pH_i record represent 3-min pauses in the acquisition of pH_i measurements to record the $[\text{Ca}^{2+}]_i$ transients shown in the *middle panels*. *B*: percentage decreases in the peak amplitudes of $[\text{Ca}^{2+}]_i$ transients (\square) and decreases in pH_i (\bullet) observed in individual neurons on reducing pH_o from 7.2 to 6.5, plotted against percentage decreases in the peak amplitudes of the slow AHPs observed in the same cells. Low pH_o -induced decrease in the $[\text{Ca}^{2+}]_i$ transient, but not the low pH_o -induced decrease in pH_i , was significantly correlated with the inhibition of the slow AHP ($P < 0.01$ and $P = 0.17$, respectively, as determined by a *t*-test of the Pearson product-moment correlation coefficient for each data set). Solid line is a linear least-squares regression fit to the data points (\square) relating the percentage decrease in the slow AHP to the percentage decrease in the $[\text{Ca}^{2+}]_i$ transient ($r^2 = 0.97$).

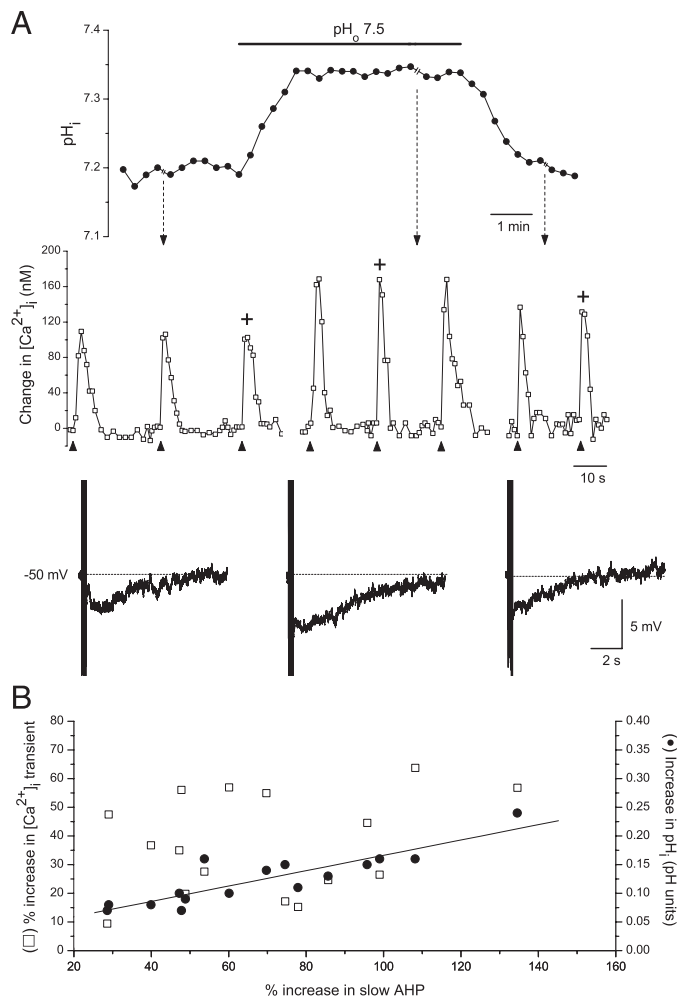


FIG. 6. Effects of an increase in pH_o on pH_i , $[Ca^{2+}]_i$ transients, and the slow AHP. *A*: simultaneous measurements of pH_i (top), $[Ca^{2+}]_i$ (middle), and V_m (bottom) from a perforated patch-clamped hippocampal neuron under HCO_3^-/CO_2 -buffered conditions. Increasing pH_o from 7.2 to 7.5 increased pH_i . Peak amplitudes of $[Ca^{2+}]_i$ transients (evoked by trains of 13 action potentials applied at \blacktriangle) and the subsequent slow AHPs were increased at pH_o 7.5 compared with pH_o 7.2. Breaks in the pH_i record represent 2-min (at pH_o 7.2) and 3-min (at pH_o 7.5) pauses in the acquisition of pH_i measurements to record the $[Ca^{2+}]_i$ transients shown in the middle panels. *B*: percentage increases in the peak amplitudes of $[Ca^{2+}]_i$ transients (□) and increases in pH_i (●) observed in individual neurons on increasing pH_o from 7.2 to 7.5, plotted against percentage increases in the peak amplitudes of the slow AHPs observed in the same cells. High pH_o -induced augmentation of the slow AHP was significantly correlated with the increase in pH_i but not the increase in the $[Ca^{2+}]_i$ transient ($P < 0.01$ and $P = 0.26$, respectively, as determined by a t -test of the Pearson product-moment correlation coefficient for each data set). Solid line is a linear least-squares regression fit to the data points (●) relating the percentage increase in the slow AHP to the increase in pH_i ($r^2 = 0.97$).

change pH_i at a constant pH_o , at above ambient temperature they produce only transient changes in pH_i in hippocampal neurons (Bonnet et al. 2000; Church et al. 1998). In addition, NH_3 and trimethylamine directly inhibit the slow AHP and sI_{AHP} in rat hippocampal neurons (Kelly and Church 2004, 2005). In light of these considerations, we used the transition from a nominally HCO_3^-/CO_2 -free HEPES-buffered medium to a HCO_3^-/CO_2 -buffered medium (pH_o constant at 7.2) to change pH_i at a constant pH_o . As described by Brett et al. (2002) (see also Bevensee et al. 1996; Smith et al. 1998), the addition of HCO_3^- activates HCO_3^- -dependent pH_i -regulating

mechanisms such that, in neurons with a low resting pH_i in the absence of HCO_3^- , Na^+ -dependent Cl^-/HCO_3^- exchange causes pH_i to rise, whereas in neurons with a high resting pH_i in the absence of HCO_3^- , Na^+ -independent Cl^-/HCO_3^- exchange causes pH_i to fall.

Consistent with the findings of Brett et al. (2002) in intact hippocampal neurons, switching from a HCO_3^- -free to a HCO_3^- -containing medium (pH_o constant at 7.2) caused pH_i to decrease in 11 of 13 perforated patch-clamped neurons with high (>7.14) initial pH_i values in HCO_3^- -free medium (of the remaining neurons, one showed no change and the other a small increase in pH_i) and to increase in three of three neurons with low (≤ 7.14) initial pH_i values in HCO_3^- -free medium (Fig. 7). The addition of HCO_3^- failed to significantly affect resting $[Ca^{2+}]_i$, which was 86 ± 3 nM in the absence and 90 ± 3 nM in the presence of HCO_3^- ($P > 0.8$; see also Ou-Yang et al. 1994a,b).

As illustrated in Fig. 8, *A* and *B*, changes in pH_i at a constant pH_o produced only minor changes in the peak amplitudes of depolarization-evoked $[Ca^{2+}]_i$ transients (see also Church et al. 1998) but consistently altered the peak amplitudes of the subsequent slow AHPs. When the percentage changes in the peak amplitudes of $[Ca^{2+}]_i$ transients and the changes in pH_i observed in individual neurons on the addition of HCO_3^- (pH_o constant at 7.2) were plotted against the percentage changes in the peak amplitudes of the slow AHPs measured in the same cells (Fig. 8*C*), the percentage change in the slow AHP was significantly ($P < 0.01$) correlated with the change in pH_i but not with the change in the peak amplitude of the preceding $[Ca^{2+}]_i$ transient ($P = 0.59$). The same results were obtained

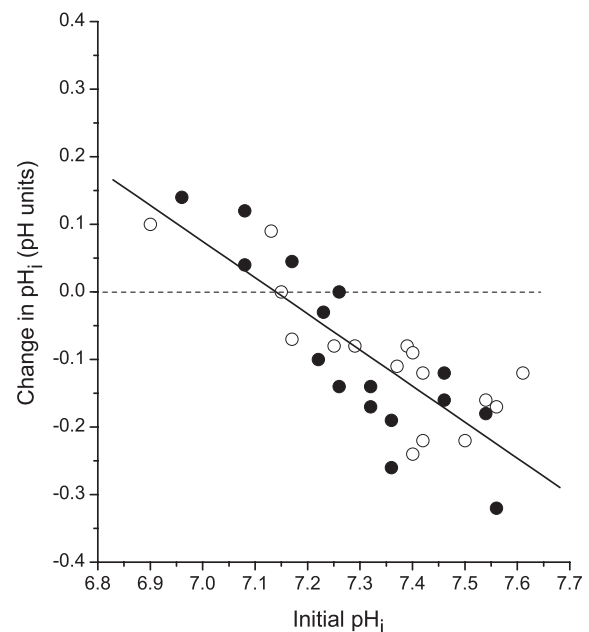


FIG. 7. Changes in pH_i evoked by the transition from a HCO_3^-/CO_2 -free to a HCO_3^-/CO_2 -containing medium at a constant pH_o . Changes in steady-state pH_i observed in patch-clamped (●) and neighboring intact neurons on the same coverslips (○) on the transition from a pH 7.2 HCO_3^- -free medium to a pH 7.2 HCO_3^- -containing medium are plotted against initial pH_i values in HCO_3^- -free medium. Separate linear least-squares regression fits to the data obtained from patch-clamped and intact neurons were not significantly different ($P > 0.05$) and all data points were best fit ($r^2 = 0.83$) by a single linear least-squares regression fit (solid line) that had a negative slope and an x -intercept at pH_i 7.14.

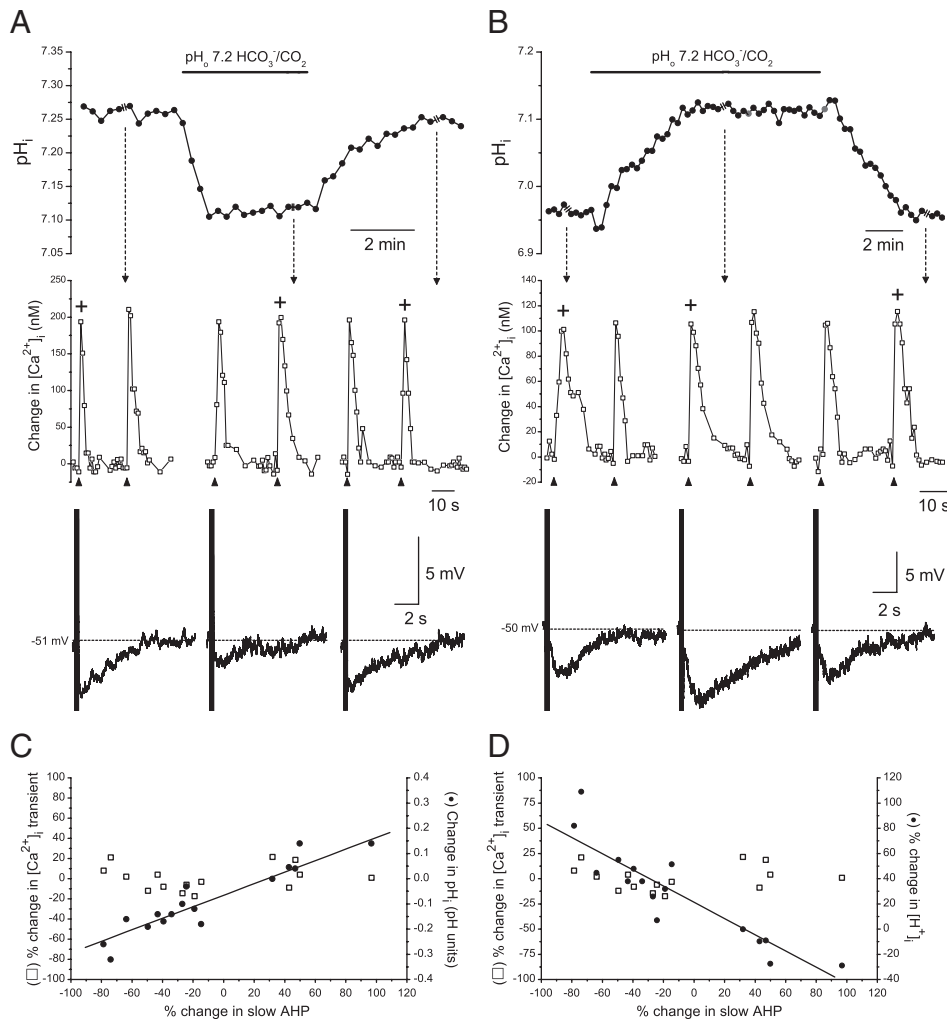


FIG. 8. Effects of changing pH_i at a constant pH_o on depolarization-evoked $[\text{Ca}^{2+}]_i$ transients and the slow AHP. *A* and *B*: simultaneous measurements of pH_i (top), $[\text{Ca}^{2+}]_i$ (middle), and V_m (bottom) in perforated patch-clamped neurons in response to the transition from a $\text{pH} 7.2 \text{ HCO}_3^-/\text{CO}_2$ -free to a $\text{pH} 7.2 \text{ HCO}_3^-/\text{CO}_2$ -buffered medium. *A*: in a neuron with a high initial pH_i (about 7.25), the addition of HCO_3^- caused pH_i to decrease. Although the reduction in pH_i at a constant pH_o had little effect on the peak amplitudes of $[\text{Ca}^{2+}]_i$ transients evoked by trains of 13 action potentials (applied at \blacktriangle), the peak amplitude of the slow AHP was reduced. *B*: in a different neuron with a low initial pH_i (about 6.95), the addition of HCO_3^- increased pH_i and concurrently augmented the slow AHP without appreciably altering the preceding $[\text{Ca}^{2+}]_i$ transient. In *A* and *B*, breaks in the pH_i records represent 2-min pauses in data acquisition to record the $[\text{Ca}^{2+}]_i$ transients shown immediately below. *C*: percentage changes in the peak amplitudes of $[\text{Ca}^{2+}]_i$ transients (\square) and changes in pH_i (\bullet) observed in individual neurons on the addition of HCO_3^- (pH_o constant at 7.2) plotted against the percentage changes in the peak amplitudes of the slow AHPs observed in the same cells. Changes in the slow AHPs were significantly correlated with the changes in pH_i but not with the changes in the preceding depolarization-evoked $[\text{Ca}^{2+}]_i$ transients ($P < 0.01$ and $P = 0.59$, respectively, as determined by a *t*-test of the Pearson product-moment correlation coefficient for each data set). Solid line is a linear least-squares regression fit to the data points (\bullet) relating the percentage change in the slow AHP to the change in pH_i ($r^2 = 0.91$). *D*: like *C*, but with change in pH_i plotted as percentage change in $[\text{H}^+]_i$. Solid line is a linear least-squares regression fit to the data points (\bullet) relating the percentage change in the slow AHP to the percentage change in $[\text{H}^+]_i$ ($r^2 = 0.88$).

when the change in pH_i was plotted as a change in $[\text{H}^+]_i$ (not shown) or as a percentage change in $[\text{H}^+]_i$ (Fig. 8D). A distinct sI_{ahp} was discernable in one neuron in this experimental series; in this cell, pH_i decreased by 0.10 pH units on the addition of HCO_3^- (pH_o constant at 7.2) and the peak amplitude of sI_{ahp} declined by 25%, from 51 pA in the absence of HCO_3^- to 38 pA in the presence of HCO_3^- .

DISCUSSION

We developed a technique to measure $[\text{Ca}^{2+}]_i$, pH_i , and V_m simultaneously in cultured hippocampal neurons and used it to substantiate and extend previous findings, made on the basis of electrophysiological recordings from CA1 pyramidal neurons in slices (Church 1992, 1999; Church and McLennan 1989; Kelly and Church 2004), that the slow AHP is modulated by changes in pH_o and pH_i . Although changes in pH_i at a constant pH_o were able to modulate the slow AHP in the absence of marked changes in $[\text{Ca}^{2+}]_i$ transients, inhibition of the slow AHP by decreases in pH_o was not dependent on reductions in pH_i but rather reflected a low pH_o -dependent reduction in the priming Ca^{2+} signal. In contrast, high pH_o -induced increases in the slow AHP appeared to reflect the accompanying increase in pH_i rather than an increase in the preceding $[\text{Ca}^{2+}]_i$ transient.

Simultaneous measurements of V_m , $[\text{Ca}^{2+}]_i$, and pH_i

Although simultaneous measurements of V_m and $[\text{Ca}^{2+}]_i$ (e.g., Abel et al. 2004; Sah and Clements 1999), V_m and pH_i (e.g., Trapp et al. 1996; Willoughby and Schwiening 2002), and pH_i and $[\text{Ca}^{2+}]_i$ (e.g., Austin et al. 1996; Martínez-Zaguilán et al. 1991) are relatively commonplace, concurrent measurements of all three parameters have for the most part been limited to larger cells (e.g., invertebrate neurons) impaled with ion-sensitive microelectrodes (ISMs) (but see Silver and Erecinska 1990). The technique described here provides a means to measure $[\text{Ca}^{2+}]_i$, pH_i , and V_m simultaneously in small cells that are not readily amenable to stable impalements with ISMs and offers a means to better understand the relationships between cytosolic $[\text{Ca}^{2+}]$ and $[\text{H}^+]$ and the roles of both ions in the regulation of cellular excitability. The validity of the technique was attested to by the facts that resting pH_i values, the distribution of resting pH_i values, and the magnitudes of the changes in pH_i evoked by changes in pH_o or the addition of external HCO_3^- in dual dye-loaded patch-clamped cells were in agreement with those obtained in previous studies where pH_i alone was measured (e.g., Brett et al. 2002; Sheldon et al. 2004a; Smith et al. 1998). In addition, resting $[\text{Ca}^{2+}]_i$ values and the amplitudes of $[\text{Ca}^{2+}]_i$ transients evoked under control ($\text{pH}_o 7.2$) conditions in perforated patch-clamped neurons

loaded with fura-2 and SNARF-5F corresponded well with those measured previously with fura-2 alone under similar stimulating (trains of action potentials, as opposed to depolarizing voltage steps) and recording (bulk cytosolic measurements at the soma) conditions (e.g., Abel et al. 2004; Church et al. 1994, 1998; Knöpfel et al. 1990; Lancaster and Batchelor 2000; Lee et al. 2005). Finally, not only were V_m and R_{in} in dual dye-loaded neurons patch-clamped using the perforated patch-clamp technique similar to values measured in unloaded cells but also the pharmacological and other characteristics of the slow AHP in dual dye-loaded neurons were comparable to those observed previously by ourselves (Kelly and Church 2004) and others (e.g., Shah and Haylett 2000; Shah et al. 2001) in the absence of fluorophore(s), provided that fura-2-AM was loaded at $\leq 1 \mu\text{M}$.

Effects of changes in pH

Although changes in pH_i are known to affect HVA Ca^{2+} currents in rat hippocampal neurons (Tombaugh and Somjen 1997), in the present study changes in pH_i at a constant pH_o modulated the slow AHP in the absence of marked changes in the priming Ca^{2+} signal. This finding is in agreement with previous conventional sharp microelectrode and whole cell recordings in CA1 neurons in slices (Church 1999; Kelly and Church 2004; see also Church et al. 1998), where reductions in the slow AHP and sI_{ahp} evoked by decreases in pH_i at a constant pH_o occurred in the absence of significant changes in Ca^{2+} -dependent depolarizing potentials or I_{Ca} and were significantly attenuated when internal buffering power was raised by the inclusion of high concentrations of H^+ buffers in the recording electrode. Also in support of pH_i being an important modulator of the slow AHP is the observation that high pH_o -induced increases in the potential were correlated with the accompanying increases in pH_i but not the accompanying increases in $[\text{Ca}^{2+}]_i$ transients. This result is also entirely consistent with previous conventional whole cell recordings from CA1 neurons in slices (Kelly and Church 2004), where in addition it was found that the effects of high pH_o to augment the slow AHP and sI_{ahp} were significantly attenuated by increasing internal H^+ buffering capacity in the absence of any change in the preceding Ca^{2+} potentials.

The apparent dissociation between the priming Ca^{2+} signal and the magnitude of the slow AHP when pH_i is changed at a constant pH_o could reflect the effects of changes in pH_i on the slow AHP and, possibly, other K^+ conductances (see Church et al. 1998) that, in turn, would act to offset any direct effect of changes in pH_i on Ca^{2+} influx, resulting in little net effect on the magnitude of $[\text{Ca}^{2+}]_i$ transients. Alternatively, the relatively small changes in pH_i used in the present experiments may have been insufficient to appreciably affect the activities of the L- and N-type HVA Ca^{2+} channels that in large part mediate depolarization-evoked increases in $[\text{Ca}^{2+}]_i$ and the subsequent activation of the slow AHP in rat hippocampal neurons (see Borde et al. 2000; Church et al. 1994, 1998; Kelly and Church 2004; Shah and Haylett 2000; Tanabe et al. 1998). Importantly, L- and N-type Ca^{2+} channels in rat hippocampal neurons exhibit similar sensitivities to changes in pH_o and pH_i (Church et al. 1998; Tombaugh and Somjen 1996, 1997), indicating that the lack of correlation between the amplitude of depolarization-evoked $[\text{Ca}^{2+}]_i$ transients and the slow AHP

when pH_o is increased or when pH_i is changed at a constant pH_o is unlikely to reflect the possibility that changes in pH_i might be affecting Ca^{2+} entry through a Ca^{2+} channel subtype that does not contribute to the activation of the slow AHP.

In agreement with previous reports (e.g., Church 1999; Church et al. 1998; Ou-Yang et al. 1994a), decreasing pH_o from 7.2 to 6.5 decreased pH_i , reduced the magnitude of depolarization-evoked $[\text{Ca}^{2+}]_i$ transients, and inhibited the subsequent slow AHPs. In contrast to results obtained at pH_o 7.5, however, the decrease in the slow AHP at pH_o 6.5 was correlated with a low pH_o -dependent decrease in the priming Ca^{2+} signal rather than a low pH_o -induced decrease in pH_i . This observation parallels previous findings in conventional whole cell patch-clamped CA1 neurons in slices (Kelly and Church 2004), where low pH_o -induced reductions in the slow AHP and sI_{ahp} were accompanied by decreases in depolarization-evoked Ca^{2+} -dependent potentials and I_{Ca} , and were not significantly affected by increasing internal H^+ buffering capacity.

The differences between the mechanisms by which reductions and increases in pH_o modulate the slow AHP may be explained by a number of factors. For example, the marked decrease in $[\text{Ca}^{2+}]_i$ transients observed at pH_o 6.5, which is consistent with the pKs for the effects of pH_o on L- and N-type HVA Ca^{2+} currents and depolarization-evoked $[\text{Ca}^{2+}]_i$ transients in rat hippocampal neurons (pH_o 7.1–7.2; Church et al. 1998; Tombaugh and Somjen 1996), may have reduced the slow AHP to such an extent that modest decreases in pH_i consequent on decreases in pH_o failed to exert an additional inhibitory effect. In contrast, the augmented slow AHP at pH_o 7.5 occurred despite the likelihood that the underlying channels were already saturated with Ca^{2+} (see Abel et al. 2004; Gerlach et al. 2004; Shah and Haylett 2000). Although this is consistent with the possibility that internal protons modulate the slow AHP by an allosteric site on the channel complex (see Laurido et al. 1991), the possibility remains that protons may compete with Ca^{2+} ions at regulatory binding sites to modulate channel activity (see Church et al. 1998; Copello et al. 1991; Kume et al. 1990; Peitersen et al. 2006). Because microdomains of $[\text{Ca}^{2+}]_i$ and/or pH_i in the immediate vicinity of the channels underlying the slow AHP may differ from values measured in bulk cytoplasm (e.g., Ro and Carson 2004; Vaughan-Jones et al. 2006; Willoughby and Schwiening 2002; Willoughby et al. 2005), simultaneous near-membrane $[\text{Ca}^{2+}]_i$ and pH_i measurements may help shed further light on the relationships between Ca^{2+} and H^+ in the regulation of the slow AHP. Nevertheless, it must be noted that the mechanism(s) whereby Ca^{2+} activates the channels underlying the slow AHP remain unknown (cf. BK- and SK-type Ca^{2+} -activated K^+ channels; see Sah and Faber 2002; Stocker 2004; Vogalis et al. 2003) and, consistent with a role for a cytoplasmic intermediate between Ca^{2+} and the gating of the channels underlying the slow AHP, activation of the slow AHP has been reported to require elevations in bulk cytosolic $[\text{Ca}^{2+}]$ rather than at the membrane (Abel et al. 2004; see also Lasser-Ross et al. 1997; Lee et al. 2005). Kinetic studies at the single-channel level will be required to determine the precise mechanism(s) whereby protons interact with Ca^{2+} ions to modulate the slow AHP.

We did not address the possibilities that changes in pH_o might act directly on the channels underlying the slow AHP or

that changes in pH_o and/or pH_i might affect processes downstream from Ca^{2+} influx that could potentially modulate the magnitude of the Ca^{2+} signal responsible for their activation. Nevertheless, changes in pH_o fail to affect the unitary properties of BK-, IK-, or SK-type Ca^{2+} -activated K^+ channels in a variety of cell types (Church et al. 1998; Jäger and Grissmer 2004; Kume et al. 1990; Pedersen et al. 2000) and, in the present study (see also Kelly and Church 2004), pH_o -induced changes in the slow AHP were never observed in the absence of parallel changes in the magnitude of $[Ca^{2+}]_i$ transients. In addition, although changes in pH_i can affect Ca^{2+} handling by intracellular stores, internal Ca^{2+} buffering, and the activities of $[Ca^{2+}]_i$ extrusion mechanisms (e.g., Hoyt and Reynolds 1998; Ou-Yang et al. 1994b; Thomas 2002; Zucker 1981), the relatively modest changes in pH_o and/or pH_i used here (also Church et al. 1998) were not associated with marked changes in resting $[Ca^{2+}]_i$ or the generation of depolarization-independent $[Ca^{2+}]_i$ transients, and changing pH_i at a constant pH_o failed to significantly affect the magnitude of depolarization-evoked $[Ca^{2+}]_i$ transients.

Functional implications

In summary, simultaneous measurements of $[Ca^{2+}]_i$, pH_i , and V_m indicate that changes in pH_o modulate the slow AHP in rat hippocampal neurons in a manner that depends on the direction of the pH_o change; moderate reductions in pH_o inhibit the slow AHP primarily by reducing Ca^{2+} influx, whereas moderate increases in pH_o augment the slow AHP primarily through an increase in pH_i . In addition, changes in pH_i at a constant pH_o modulate the slow AHP independent from changes in the priming Ca^{2+} signal, further supporting a role for pH_i in the regulation of the slow AHP.

The sensitivity of the slow AHP to the changes in pH_o and pH_i used here, which are within the pathophysiological range seen in vivo (see Chesler 2003), may have a number of implications for neuronal function. Reductions in pH, for example, may contribute to the inhibition of the slow AHP observed during oxygen deprivation (Kulik et al. 2002) and, if pronounced, may in this way promote neuronal injury. Conversely, an increase in the slow AHP may help to limit the increases in neuronal excitability and epileptiform activity observed during increases in pH (Balestrino and Somjen 1988; Church and McLennan 1989; also Kelly and Church, unpublished observations), especially if Ca^{2+} influx is increased to such an extent that the underlying channels become saturated (see Canepari et al. 2000; Sinha et al. 1995). The present results also raise the possibility that activity-induced reductions in $pH_{o/i}$ could limit the potential therapeutic effects of agents designed to enhance the slow AHP, and it will be important to assess whether such agents, like the neuronal SK channel enhancer EBIO (Peitersen et al. 2006; see also Pedarzani et al. 2005), retain their ability to augment the slow AHP at the low pH values associated with pathological events such as ischemia.

GRANTS

This work was funded by a Grant-in-Aid from the Heart and Stroke Foundation of British Columbia and Yukon and an Operating Grant from the Canadian Institutes of Health Research.

REFERENCES

- Abel HJ, Lee JCF, Callaway JC, and Foehring RC. Relationships between intracellular calcium and afterhyperpolarizations in neocortical pyramidal neurons. *J Neurophysiol* 91: 324–335, 2004.
- Alger BE, Sim JA, and Brown DA. Single-channel activity correlated with medium-duration, Ca-dependent K current in cultured rat hippocampal neurones. *Neurosci Lett* 168: 23–28, 1994.
- Austin C, Dilly K, Eisner D, and Wray S. Simultaneous measurements of intracellular pH, calcium and tension in rat mesenteric vessels: effects of extracellular pH. *Biochem Biophys Res Commun* 222: 537–540, 1996.
- Balestrino M and Somjen GG. Concentration of carbon dioxide, interstitial pH and synaptic transmission in hippocampal formation of the rat. *J Physiol* 396: 247–266, 1988.
- Baxter KA and Church J. Characterization of acid extrusion mechanisms in cultured fetal rat hippocampal neurones. *J Physiol* 493: 457–470, 1996.
- Bevensee MO, Cummins TR, Haddad GG, Boron WF, and Boyarsky G. pH regulation in single CA1 neurons acutely isolated from the hippocampi of immature and mature rats. *J Physiol* 494: 315–328, 1996.
- Bonnet U, Bingmann D, and Wiemann M. Intracellular pH modulates spontaneous and epileptiform bioelectric activity of hippocampal CA3-neurons. *Eur Neuropsychopharmacol* 10: 97–103, 2000.
- Borde M, Bonansco C, Fernández de Sevilla D, Le Ray D, and Buño W. Voltage-clamp analysis of the potentiation of the slow Ca^{2+} -activated K^+ current in hippocampal pyramidal neurons. *Hippocampus* 10: 198–206, 2000.
- Brett CL, Kelly T, Sheldon C, and Church J. Regulation of $Cl^-HCO_3^-$ exchangers by cAMP-dependent protein kinase in adult rat hippocampal CA1 neurons. *J Physiol* 545: 837–853, 2002.
- Canepari M, Mammano F, Kachalsky SG, Rahamimoff R, and Cherubini E. GABA- and glutamate-mediated network activity in the hippocampus of neonatal and juvenile rats revealed by fast calcium imaging. *Cell Calcium* 27: 25–33, 2000.
- Chesler M. Regulation and modulation of pH in the brain. *Physiol Rev* 83: 1183–1221, 2003.
- Church J. A change from $HCO_3^-CO_2$ - to HEPES-buffered medium modifies membrane properties of rat CA1 pyramidal neurones *in vitro*. *J Physiol* 455: 51–71, 1992.
- Church J. Effects of pH changes on calcium-mediated potentials in rat hippocampal neurons *in vitro*. *Neuroscience* 89: 731–742, 1999.
- Church J, Baxter KA, and McLarnon JG. pH modulation of Ca^{2+} responses and a Ca^{2+} -dependent K^+ channel in cultured rat hippocampal neurones. *J Physiol* 511: 119–132, 1998.
- Church J, Fletcher EJ, Abdel-Hamid K, and MacDonald JF. Loperamide blocks high-voltage-activated calcium channels and N-methyl-D-aspartate-evoked responses in rat and mouse cultured hippocampal pyramidal neurons. *Mol Pharmacol* 45: 747–757, 1994.
- Church J and McLennan H. Electrophysiological properties of rat CA1 pyramidal neurones *in vitro* modified by changes in extracellular bicarbonate. *J Physiol* 415: 85–108, 1989.
- Copello J, Segal Y, and Reuss L. Cytosolic pH regulates maxi K^+ channels in *Necturus* gall-bladder epithelial cells. *J Physiol* 434: 577–590, 1991.
- Gerlach AC, Maylie J, and Adelman JP. Activation kinetics of the slow afterhyperpolarization in hippocampal CA1 neurons. *Pfluegers Arch* 448: 187–196, 2004.
- Glantz SA. *Primer of Biostatistics* (5th ed.). New York: McGraw-Hill, 2002.
- Helmchen F, Imoto K, and Sakmann B. Ca^{2+} buffering and action potential-evoked Ca^{2+} signaling in dendrites of pyramidal neurons. *Biophys J* 70: 1069–1081, 1996.
- Hoyt KR and Reynolds IJ. Alkalinization prolongs recovery from glutamate-induced increases in intracellular Ca^{2+} concentration by enhancing Ca^{2+} efflux through the mitochondrial Na^+/Ca^{2+} exchanger in cultured rat forebrain neurons. *J Neurochem* 71: 1051–1058, 1998.
- Jäger H and Grissmer S. Characterization of the outer pore region of the apamin-sensitive Ca^{2+} -activated K^+ channel rSK2. *Toxicon* 43: 951–960, 2004.
- Kelly T and Church J. pH modulation of currents that contribute to the medium and slow afterhyperpolarizations in rat CA1 pyramidal neurones. *J Physiol* 554: 449–466, 2004.
- Kelly T and Church J. The weak bases NH_3 and trimethylamine inhibit the medium and slow afterhyperpolarizations in rat CA1 pyramidal neurones. *Pfluegers Arch* 451: 418–427, 2005.
- Knöpfel T, Vranesic I, Gähwiler BH, and Brown DA. Muscarinic and β -adrenergic depression of the slow Ca^{2+} -activated potassium conductance

- in hippocampal CA3 pyramidal cells is not mediated by a reduction of depolarization-induced cytosolic Ca^{2+} transients. *Proc Natl Acad Sci USA* 87: 4083–4087, 1990.
- Kulik A, Brockhaus J, Pedarzani P, and Ballanyi K.** Chemical anoxia activates ATP-sensitive and blocks Ca^{2+} -dependent K^+ channels in rat dorsal vagal neurons *in situ*. *Neuroscience* 110: 541–554, 2002.
- Kume H, Takagi K, Satake T, Tokuno H, and Tomita T.** Effects of intracellular pH on calcium-activated potassium channels in rabbit tracheal smooth muscle. *J Physiol* 424: 445–457, 1990.
- Lancaster B and Batchelor AM.** Novel action of BAPTA series chelators on intrinsic K^+ currents in rat hippocampal neurones. *J Physiol* 522: 231–246, 2000.
- Lasser-Ross N, Ross WN, and Yarom Y.** Activity-dependent $[\text{Ca}^{2+}]_i$ changes in guinea pig vagal motoneurons: relationship to the slow afterhyperpolarization. *J Neurophysiol* 78: 825–834, 1997.
- Laurido C, Candia S, Wolff D, and Latorre R.** Proton modulation of a Ca^{2+} -activated K^+ channel from rat skeletal muscle incorporated into planar bilayers. *J Gen Physiol* 98: 1025–1043, 1991.
- Lee JCF, Callaway JC, and Foehring RC.** Effects of temperature on calcium transients and Ca^{2+} -dependent afterhyperpolarizations in neocortical pyramidal neurons. *J Neurophysiol* 93: 2012–2020, 2005.
- Martínez-Zaguilán R, Gurulé MW, and Lynch RM.** Simultaneous measurement of intracellular pH and Ca^{2+} in insulin-secreting cells by spectral imaging microscopy. *Am J Physiol Cell Physiol* 270: C1438–C1446, 1996a.
- Martínez-Zaguilán R, Martínez GM, Lattanzio F, and Gillies RJ.** Simultaneous measurement of intracellular pH and Ca^{2+} using the fluorescence of SNARF-1 and fura-2. *Am J Physiol Cell Physiol* 260: C297–C307, 1991.
- Martínez-Zaguilán R, Parnami G, and Lynch RM.** Selection of fluorescent ion indicators for simultaneous measurements of pH and Ca^{2+} . *Cell Calcium* 19: 337–349, 1996b.
- Ou-Yang YB, Kristián T, Mellergård P, and Siesjö BK.** The influence of pH on glutamate- and depolarization-induced increases of intracellular calcium concentration in cortical neurons in primary culture. *Brain Res* 646: 65–72, 1994a.
- Ou-Yang YB, Mellergård P, Kristián T, Kristiánova V, and Siesjö BK.** Influence of acid-base changes on the intracellular calcium concentration of neurons in primary culture. *Exp Brain Res* 101: 265–271, 1994b.
- Pedarzani P, McCutcheon JE, Rogge G, Jensen BS, Christophersen P, Hougaard C, Strobaek D, and Stocker M.** Specific enhancement of SK channel activity selectively potentiates the afterhyperpolarizing current I_{ahp} and modulates the firing properties of hippocampal pyramidal neurons. *J Biol Chem* 280: 41404–41411, 2005.
- Pedersen KA, Jørgensen NK, Jensen BS, and Olesen S-P.** Inhibition of the human intermediate-conductance, Ca^{2+} -activated K^+ channel by intracellular acidification. *Pfluegers Arch* 440: 153–156, 2000.
- Peitersen T, Hougaard C, Jespersen T, Jørgensen NK, Olesen S-P, and Grunnet M.** Subtype-specific, bi-component inhibition of SK channels by low internal pH. *Biochem Biophys Res Commun* 343: 943–949, 2006.
- Ro HA and Carson JH.** pH microdomains in oligodendrocytes. *J Biol Chem* 279: 37115–37123, 2004.
- Sah P and Clements JD.** Photolytic manipulation of $[\text{Ca}^{2+}]_i$ reveals slow kinetics of potassium channels underlying the afterhyperpolarization in hippocampal pyramidal neurons. *J Neurosci* 19: 3657–3664, 1999.
- Sah P and Faber ESL.** Channels underlying neuronal calcium-activated potassium currents. *Prog Neurobiol* 66: 345–353, 2002.
- Segal M and Barker JL.** Rat hippocampal neurons in culture: Ca^{2+} and Ca^{2+} -dependent K^+ conductances. *J Neurophysiol* 55: 751–766, 1986.
- Shah M and Haylett DG.** Ca^{2+} channels involved in the generation of the slow afterhyperpolarization in cultured rat hippocampal pyramidal neurons. *J Neurophysiol* 83: 2554–2561, 2000.
- Shah MM, Miscony Z, Javadzadeh-Tabatabaie M, Ganellin CR, and Haylett DG.** Clotrimazole analogues: effective blockers of the slow afterhyperpolarization in cultured rat hippocampal pyramidal neurones. *Br J Pharmacol* 132: 889–898, 2001.
- Sheldon C, Cheng YM, and Church J.** Concurrent measurements of the free cytosolic concentrations of H^+ and Na^+ ions with fluorescent indicators. *Pfluegers Arch* 449: 307–318, 2004a.
- Sheldon C, Diarra A, Cheng YM, and Church J.** Sodium influx pathways during and after anoxia in rat hippocampal neurons. *J Neurosci* 24: 11057–11069, 2004b.
- Silver IA and Erecinska M.** Intracellular and extracellular changes of $[\text{Ca}^{2+}]_i$ in hypoxia and ischemia in rat brain *in vivo*. *J Gen Physiol* 95: 837–866, 1990.
- Sinha SR, Patel SS, and Saggau P.** Simultaneous optical recording of evoked and spontaneous transients of membrane potential and intracellular calcium concentration with high spatio-temporal resolution. *J Neurosci Methods* 60: 49–60, 1995.
- Smith GAM, Brett CL, and Church J.** Effects of noradrenaline on intracellular pH in acutely dissociated adult rat hippocampal CA1 neurones. *J Physiol* 512: 487–505, 1998.
- Stocker M.** Ca^{2+} -activated K^+ channels: molecular determinants and function of the SK family. *Nat Rev Neurosci* 5: 758–770, 2004.
- Storm JF.** Potassium currents in hippocampal pyramidal cells. *Prog Brain Res* 83: 161–187, 1990.
- Tanabe M, Gähwiler BH, and Gerber U.** L-type Ca^{2+} channels mediate the slow Ca^{2+} -dependent afterhyperpolarization current in rat CA3 pyramidal cells *in vitro*. *J Neurophysiol* 80: 2268–2273, 1998.
- Thomas RC.** The effects of HCl and CaCl_2 injections on intracellular calcium and pH in voltage-clamped snail (*Helix aspersa*) neurons. *J Gen Physiol* 120: 567–579, 2002.
- Tombaugh GC and Somjen GG.** Effects of extracellular pH on voltage-gated Na^+ , K^+ and Ca^{2+} currents in isolated rat CA1 neurons. *J Physiol* 493: 719–732, 1996.
- Tombaugh GC and Somjen GG.** Differential sensitivity to intracellular pH among high- and low-threshold Ca^{2+} currents in isolated rat CA1 neurons. *J Neurophysiol* 77: 639–653, 1997.
- Trapp S, Lückermann M, Kaila K, and Ballanyi K.** Acidosis of hippocampal neurones mediated by a plasmalemmal $\text{Ca}^{2+}/\text{H}^+$ pump. *Neuroreport* 7: 2000–2004, 1996.
- Vaughan-Jones RD, Spitzer KW, and Swietach P.** Spatial aspects of intracellular pH regulation in heart muscle. *Prog Biophys Mol Biol* 90: 207–224, 2006.
- Vogalis F, Storm JF, and Lancaster B.** SK channels and the varieties of slow after-hyperpolarizations in neurons. *Eur J Neurosci* 18: 3155–3166, 2003.
- Willoughby D, Masada N, Crossthwaite AJ, Ciruela A, and Cooper DMF.** Localized Na^+/H^+ exchanger 1 expression protects Ca^{2+} -regulated adenylyl cyclases from changes in intracellular pH. *J Biol Chem* 280: 30864–30872, 2005.
- Willoughby D and Schwiening CJ.** Electrically evoked dendritic pH transients in rat cerebellar Purkinje cells. *J Physiol* 544: 487–499, 2002.
- Wu WW, Chan CS, and Disterhoft JF.** Slow afterhyperpolarization governs the development of NMDA receptor-dependent afterdepolarization in CA1 pyramidal neurons during synaptic stimulation. *J Neurophysiol* 92: 2346–2356, 2004.
- Zucker RS.** Cytoplasmic alkalization reduces calcium buffering in molluscan central neurons. *Brain Res* 225: 155–170, 1981.